Earthquake Research in China

Volume 30, Number 3, 2016

The Time-frequency Characteristic of a Large Volume Airgun Source Wavelet and Its Influencing Factors[1]

Xia Ji[1,2], Jin Xing[1,2,3], Cai Huiteng[3], and Xu Jiajun[3]

1) Institute of Engineering Mechanics, China Earthquake Administration, Harbin 150080, China
2) Key Laboratory of Earthquake Engineering and Engineering Vibration, Institute of Engineering Mechanics, CEA, Harbin 150080, China
3) Earthquake Administration of Fujian Province, Fuzhou 350003, China

Through analyzing the near-field hydrophone records of the airgun experiment in the Jiemian reservoir, Fujian, we study the time-frequency characteristic of airgun source wavelet and the influence of gun depth and firing pressure, and explain the process of bubble oscillation based on the Johnson (1994) bubble model. The data analysis shows that: (1) Airgun wavelet is composed of primary pulse and bubble pulse. The primary pulse, which is of large amplitude, short duration and wide frequency band, is usually used in shallow exploration. The bubble pulse, which is concentrated in the low-frequency range, is usually used in deep exploration with deep vertical penetration and far horizontal propagation. (2) The variation of primary pulse amplitude with gun depth is very small, bubble pulse amplitude and the dominant frequency increase, and peak-bubble ratio and bubble period decrease. When the gun depth is 10m, primary pulse amplitude and peak-bubble ratio are maximum, which is suitable for shallow exploration; when gun depth is 25m, bubble pulse amplitude is large, and peak-bubble ratio is minimum, which is suitable for deep exploration. (3) The primary pulse amplitude, bubble pulse amplitude, peak-bubble ratio, and bubble period increase and the dominant frequency decreases with increased firing pressure.

Key words: Airgun wavelet Time-frequency characteristic Wavelet parameters Gun depth Firing pressure

[1] Received on March 29, 2016; revised on May 4, 2016. This project was jointly sponsored the Special Fund for Earthquake Scientific Research of China Earthquake Administration (2015419015), and the National Natural Sciences Foundation of China (41474071).

INTRODUCTION

An airgun source has the advantages of stable performance, high degree of automation, low cost, easy operation and control, repeatability, high accuracy, and non-pollution, and it has been applied to offshore oil exploration with great success. Relevant research has become one of the significant achievements in offshore oil exploration in the end of 20th century. Airguns are generally used as seismic source in seismic explorations in onshore-offshore transitional zones, inland lakes, offshore OBS and deep-sea streamer exploration (He Hanyi, 2001). A large-volume airgun source wavelet contains rich low-frequency components, and by repeated excitation and stacking of the signals, the signal-to-noise ratio can be increased, so the airgun source can be used for deep structure detection. Joint explorations were conducted by seismologists using offshore an airgun array seismic source in combination with seismic stations inland, and good results have been obtained in the research of deep structure exploration. Successful examples of onshore-offshore seismic explorations using airgun source include: the British BIRPS project, French ECORS, the US LARSE, New Zealand's SIGHT project, the Mona Lisa project conducted jointly by Germany, UK, Denmark and Sweden, and Japan's onshore-offshore seismic survey project in the eastern East China Sea trough (Woods, 1995; Okaya et al., 2002; Luo Guichun et al., 2006). Deep structure survey experiments using large-volume airguns as a seismic source were also conducted in China, such as the onshore-offshore deep seismic survey in the northeastern South China Sea, the airgun excitation experiment in the Shangguanhu reservoir, Hebei Province, and the land-sea joint seismic survey in the land area of Fujian and western Taiwan Straits. (Qiu Xuelin et al., 2003; Lin Jianmin, 2008; Tang Jie, 2008).

Taking the advantage of the high degree of repeatability and in combination with the high-precision observation system, the use of an airgun source can continuously monitor the velocity variations of underground mediums, thus providing a new train of thought for active monitoring of velocity and stress change in a subsurface medium and for carrying out medium property-based earthquake prediction. Related research has been conducted by scientists in the US and Turkey (Brenguier et al., 2008). Airgun source excitation experiments have been carried out by the Chinese seismologists in the Shangguanhu reservoir in Hebei, Dayingdian reservoir in Yunnan and Hutubi reservoir in Xinjiang, to monitor the velocity variation in the underground medium (Wang Weitao, 2009; Wang Baoshan et al., 2011, 2013; Yang Wei, 2013; Yang Wei et al., 2013).

In order to study the characteristics of a large-volume airgun source, the Earthquake Administration of Fujian Province carried out a large-volume airgun source excitation experiment in November, 2014 in the Jiemian reservoir in Banmian township, Youxi County, Sanming City, Fujian Province (25.926°N, 118.057°E). With the tests under different operating conditions, influencing factors such as gun depth, firing pressure, gun number, gun array size, water depth, etc. on the characteristics of airgun source wavelet were investigated. This paper presents an overview of the airgun source experiment in the Jiemian reservoir, and based on the near-field hydrophone records of the airgun experiment, analyzes the time-frequency characteristic of the airgun source wavelet and the influence of gun depth and firing pressure, and explains the process of bubble oscillation based on Johnson's bubble model (1994).

1 OVERVIEW OF THE AIRGUN SOURCE EXPERIMENT IN JIEMIAN RESERVOIR

In November, 2014, the Earthquake Administration of Fujian Province carried out a large-volume airgun excitation experiment in the Jiemian Reservoir (25.926°N, 118.057°E) which has a total capacity of 1.824 billionm^3. To get to the high-energy low-frequency signals that meet

the demand for deep exploration, we chose four 1500LL type Bolt guns to form an airgun array. A single airgun volume is 2000in^3, and the airgun array volume is 8000in^3, firing pressure is 2000psi. The airgun array is shown in Fig. 1 (a), in which airgun A and B compose sub-array 1, C and D compose sub-array 2, sub-array 1 and 2 together constitute the airgun array. The gun tray is shown in Fig. 1(b), the tray is at 2m directly above each airgun, on which the near-field hydrophone and pressure sensor are fixed to record the near-field wavelet and gun pressure signal of each gun. The near-field hydrophone sampling rate is 1000Hz, the record length of each shot is 0.5s, gun pressure sensor sampling rate is 10000Hz, and record length is 0.05s per each gun firing.

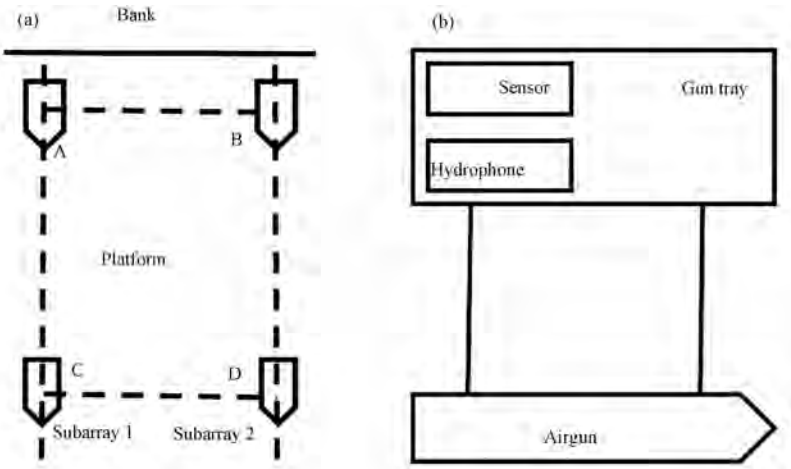

Fig. 1
Sketch of the airgun array and gun tray
(a) Airgun array; (b) Gun tray

2 TIME-FREQUENCY CHARACTERISTICS OF THE AIRGUN SOURCE WAVELET

2.1 Airgun Source Wavelet Parameters

High-pressure gas, when released into and surrounded by surrounding water, becomes a nearly spherical bubble which oscillates continuously until its attenuation and rupture, forming a series of wavelet pulses. Airgun wavelet is composed of primary pulse and bubble pulse. For the far-field wavelet, because the surface reflection coefficient is −1 theoretically, a negative ghost pulse will form immediately after the positive pulse. Wavelet parameters include the primary pulse amplitude, bubble pulse amplitude, peak-bubble ratio and bubble period. Fig. 2 is a schematic diagram of airgun wavelet.

(1) Primary pulse: Primary pulse refers to the first positive pressure pulse generated by high-pressure gas released into the water from an airgun. The primary pulse has high energy, wide bandwidth and high frequency, and is usually used in shallow oil exploration, with amplitude as bar·m. The meaning of bar·m is: taking the sound pressure value at 1m away from the epicenter as the measuring unit to measure the magnitude of the airgun pressure pulse energy. The primary pulse amplitude is closely related to the volume and firing pressure of the airgun, which are the parameters describing airgun array's energy, the greater the value, the stronger the energy released from the airgun. Usually, the larger the airgun capacity, the greater the firing pressure, the stronger the energy produced, and the greater the amplitude of the primary pulse.

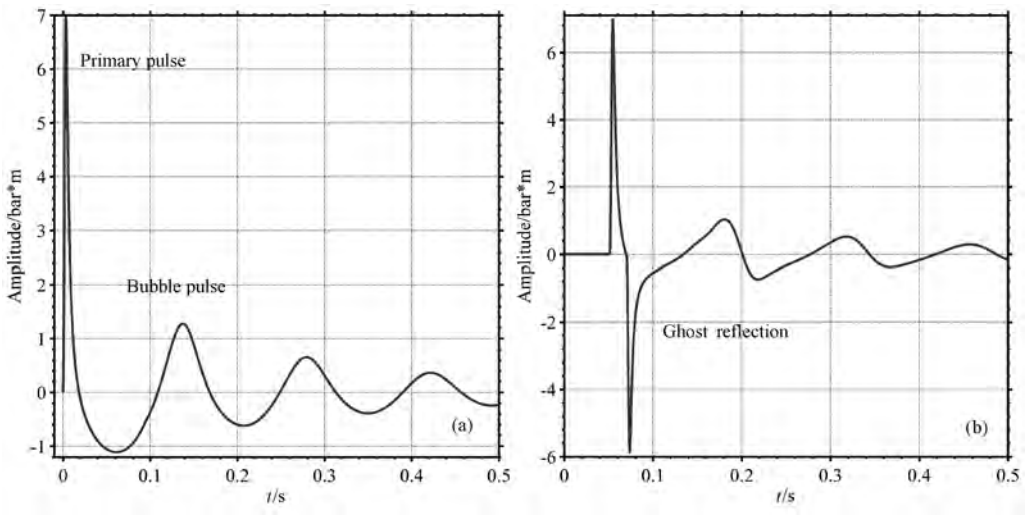

Fig. 2
Schematic diagram of airgun wavelet
(a) Near-field wavelet; (b) Far-field wavelet

The primary pulse amplitude A is expressed by the following empirical formula (He Hanyi, 2001).

$$A = C_1 V^{\frac{1}{3}} P^{\frac{3}{4}} \tag{1}$$

where, C_1 is a constant, V is for airgun volume, and P is the firing pressure.

(2) Bubble pulse: Bubble pulses are produced by oscillation of bubbles caused by high-pressure gas releasing into the water. Bubble oscillation energy concentrates mainly in the low frequency bands. Since bubble oscillation could affect the signal resolution, we need to reduce the bubble effect in shallow seismic exploration. Meanwhile, in deep seismic exploration, seismic waves are expected to penetrate deeply and propagate farther, this would require adequate low frequency energy, therefore it is necessary to enhance the bubble effect. The degree of the bubble effect is related to airgun volume, firing pressure, gun depth and array mode.

(3) Peak-bubble ratio: Peak-bubble ratio refers to the ratio of the primary pulse amplitude to the amplitude of the first bubble pulse. The bigger the peak-bubble ratio is, the wider the larger airgun wavelet frequency band, and the smoother the spectrum will be. In shallow exploration, the peak-bubble ratio is usually more than 10. Peak-bubble ratio decreases with increased gun depth and increases with increased cube root of airgun volume. Peak-bubble ratio P_b is expressed by the following empirical formula (He Hanyi, 2001).

$$P_b = \frac{C_2}{\left[34.73D\left(\frac{PV}{D+10}\right)^{-1/3} - 1\right]^{1/2} + 0.2} \tag{2}$$

where, C_2 is a constant, and D is the gun depth.

(4) Bubble period: Bubble period refers to the time interval between the main bubble and the first bubble pulse. Bubble period corresponds to the primary frequency in the low-frequency range and is closely related to airgun volume, firing pressure and gun depth. Bubble period T can be expressed by the following empirical formula (He Hanyi, 2001)

$$T = C_3 \frac{P^{\frac{1}{3}} V^{\frac{1}{3}}}{(D+10)^{\frac{5}{6}}} \tag{3}$$

where, C_3 is a constant.

2.2 Time-frequency Characteristics of the Near-field Hydrophone Records

Using the short-time Fourier transform (STFT), we analyze the time-frequency characteristics of the near-field hydrophone records of the airgun source experiment. Fig. 3 shows the time-frequency analysis of the observed waveforms recorded by near-field hydrophone in a single excitation of Gun A under the operating conditions of firing pressure 2000psi, gun depth 15m and water depth 45m, with a frequency range of 0 – 500Hz. Fig. 3(a) is the time-frequency spectrum, it is clear that in time domain 0 – 0.1s, the primary pulse concentrates in the frequency band 0 – 300Hz of the frequency domain; it has short duration, wide bandwidth and approximately uniform energy distribution at 0 – 300Hz; and in the time domain of 0.15 – 0.50s and frequency domain of 0 – 10Hz, there are 3 corresponding bubble pulses with obvious energy distribution. In the frequency of 50Hz, there is obvious energy distribution. Meanwhile, clear noise interference with a period of 0.02s can be observed in the time-domain waveform in Fig. 3(c). Considering the AC frequency of 50Hz in China, it is inferred that the energy distribution at the frequency of 50Hz is possibly the current noise; As is seen from the spectrum in Fig. 3(b), the spectrum of hydrophone records is not smooth due to the noise interference, there are many current spikes and the noise interference is evident at the frequency of 50Hz. The primary pulse in the time-domain waveform in Fig. 3(c) is very obvious, but the bubble pulse is not so clear due to the relatively small amplitude and interference of current noise. According to the time-frequency analysis in Fig. 3, time-frequency filtering is done on the near-field hydrophone records, with the primary pulse of 0.05 – 0.10s and 0 – 300Hz, and the bubble pulses in 0.1 – 0.5s and 0 – 15Hz retained, and the noises of the rest are removed; the filtering is extended to the records in the range of 0 – 100Hz (Fig. 4). It is observed from Fig. 4(a) that 50Hz current noise doesn't exist after the time-frequency filtering. The spectrum in Fig. 4(b) depresses obviously at the frequency of 50Hz, the noise spikes have been filtered, so, generally, the spectrum is smooth. There are obvious bubble pulses observed in the time-domain waveform in Fig. 4(c).

3 THE INFLUENCING FACTORS ON AIRGUN WAVELETS

3.1 Gun Depth

Gun depth is one of the key factors affecting the airgun wavelet. Gun depth has direct impact on hydrostatic pressure and ghost reflection of water surface, thereby affecting the high-pressure gas release rate, the bubble oscillation and the wavelet waveform. To explore the influence of gun depth on airgun source wavelets, under the operation conditions of firing pressure 2000psi and water depth 45m, we have made an experiment on the operation condition for Gun A with gun depth 8m, 10m, 12m, 15m, 18m, 20m, 25m and 30m respectively, in each operating condition, the airgun is fired nine times, time-frequency filtering is done on the waveforms of each excitation, then, the wavelet parameters are averaged and normalized for comparison. Table 1 shows the near-field airgun wavelet parameters at different gun depths. The analysis of near-field hydrophone data at different gun depths is shown in Fig. 5. Figs. 5(a), (b) are the near-field wavelet waveform and spectrum of the first excitation of gun A at gun depth 8m, 10m, 12m, 15m, 18m, 20m, 25m, and 30m, successively from top to bottom. It can be seen that with the increase of gun depth, the primary pulse waveform is consistent, and there is a great difference between the bubble pulse waveforms. With the gradual decrease of the bubble period, the first dominant frequency in the low frequency range increases gradually. Fig. 5(c) is the comparison

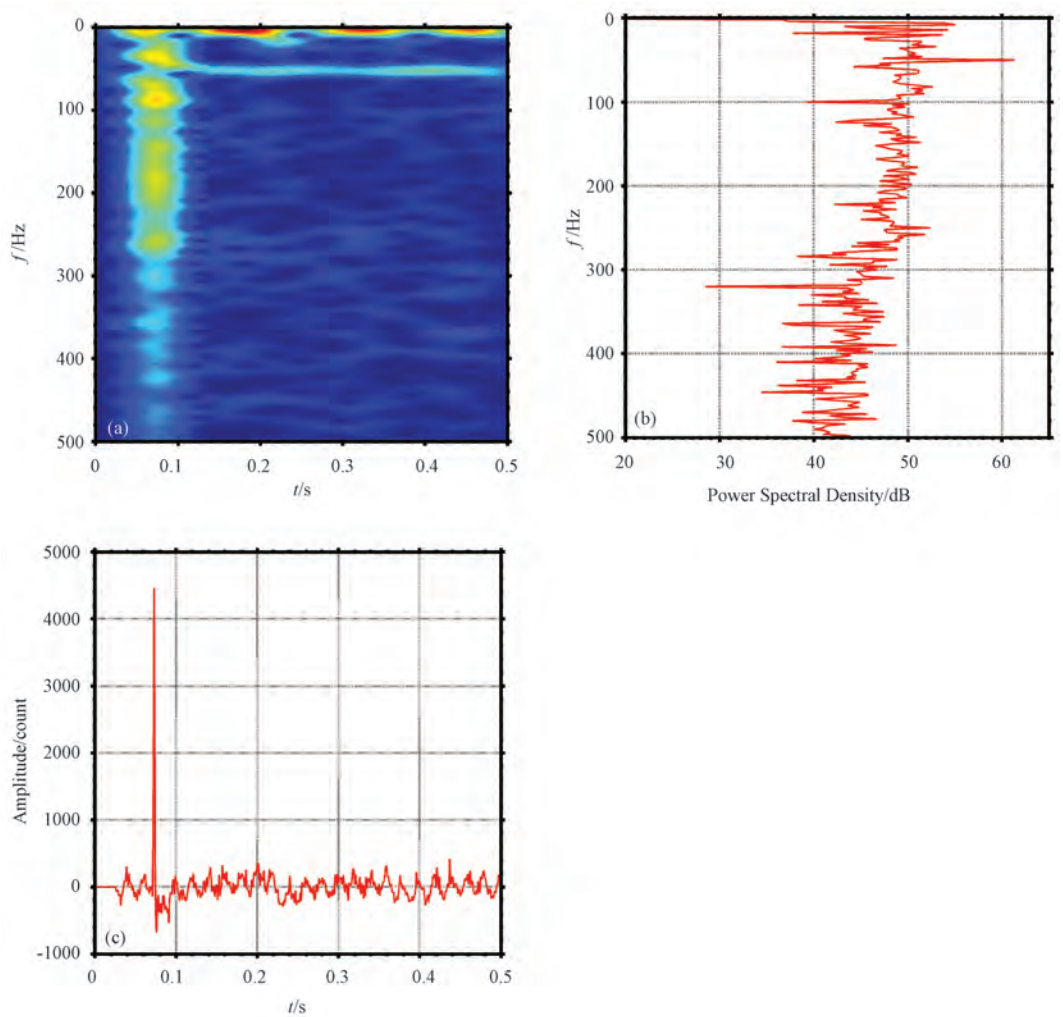

Fig. 3

Time-frequency analysis of the near-field hydrophone record

(a) Time-frequency spectrum; (b) Frequency-domain record; (c) Time-domain waveform

of correlations of near-field wavelet waveform at different gun depths, where we can see that the max cross-correlation coefficient of the primary pulse waveform (0 – 0.1s segment) is 0.9002 – 1.0000, and the correlation is high between different gun depths. The max cross-correlation coefficient of bubble pulse waveform (0.1s – 0.5s segment) is 0.3734 – 1.0000, the correlation is low between different gun depths. The max cross-correlation coefficient of airgun wavelet waveform (0 – 0.5s segment) is 0.7273 – 1.0000, and the correlation is between the primary pulse and the bubble pulse. Fig. 5(d) shows the comparison wavelet parameters after normalization. It can be seen that with increasing gun depth, the primary pulse's oscillation amplitude becomes smaller, but the range of the change is small, and the normalized value is from 0.82 to 1.15. Due to the gun depth increase, the hydrostatic pressure increases, thereby leading to the decrease of release rate of high pressure gas and the primary pulse amplitude decreases, the waveform widens and the band narrows. Since the hydrostatic pressure is small compared to the firing pressure, the amplitude of change of primary pulse is small.

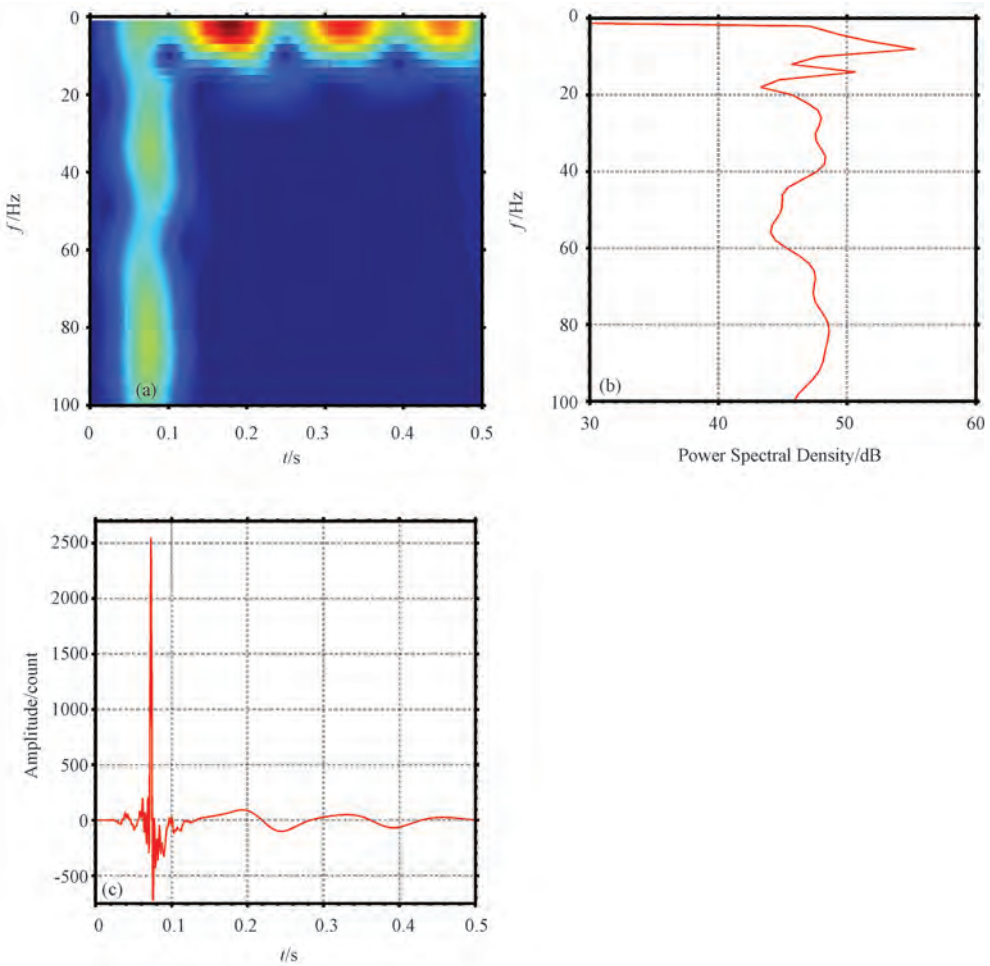

Fig. 4

Time-frequency analysis of the near-field hydrophone record after the filtering
(a) Time-frequency spectrum; (b) Frequency-domain record; (c) Time-domain waveform

Table 1 Parameters of near-field airgun wavelet at different gun depths

Gun depth/m	Wavelet parameters				
	Amplitude of primary pulse /count	Amplitude of bubble pulse /count	Peak-bubble ratio	Bubble period/s	Dominant frequency/Hz
8	1848	79. 16	23. 345	0. 166	6
10	2120	75. 37	28. 128	0. 157	6
12	1850	81. 09	22. 814	0. 140	6
15	1590	76. 16	20. 877	0. 119	6
18	1520	87. 88	17. 296	0. 109	8
20	1674	97. 58	17. 155	0. 098	8
25	1516	110. 40	13. 732	0. 084	10
30	1587	110. 70	14. 336	0. 062	10

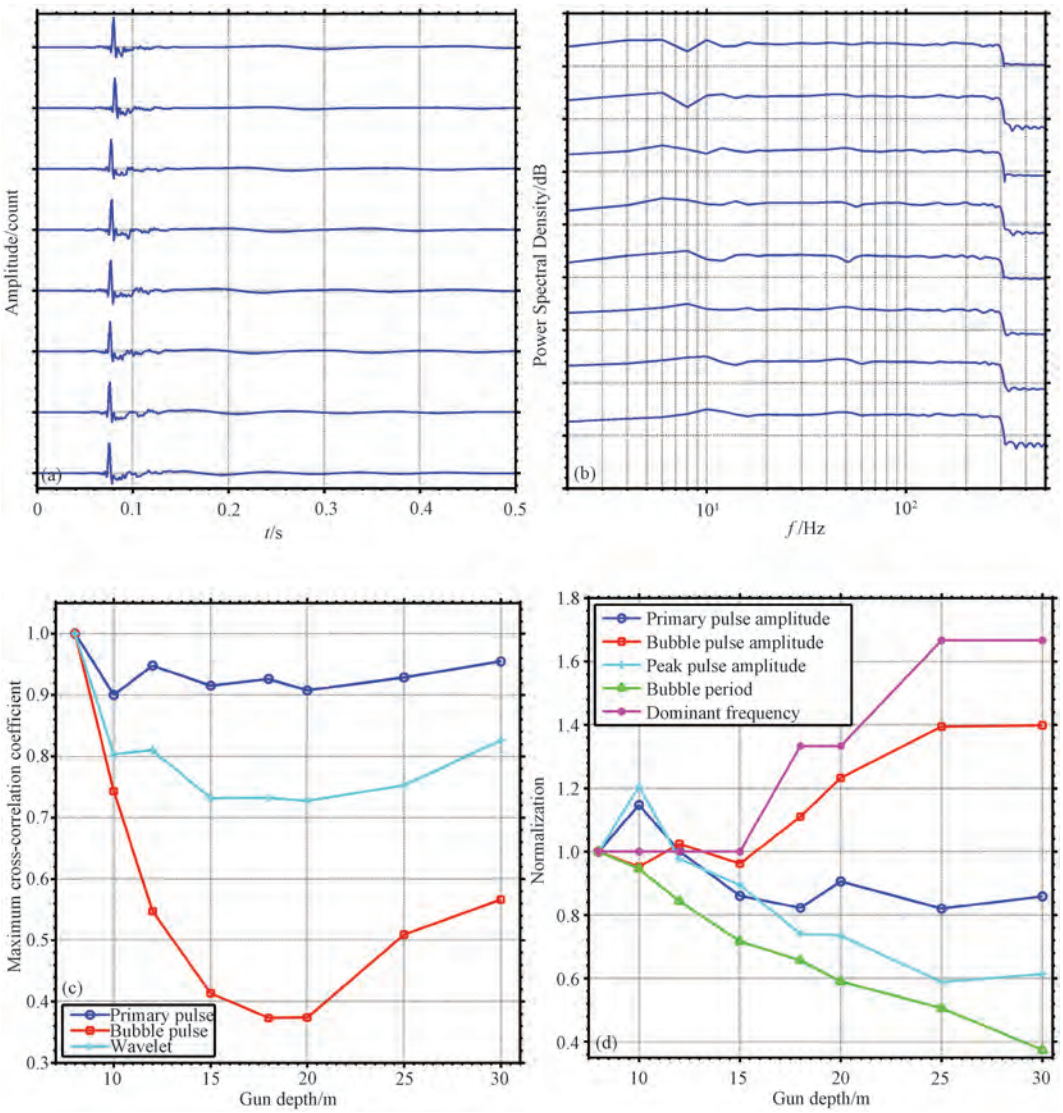

Fig. 5

Analysis of near-field hydrophone records at different gun depths

(a) Time-domain waveforms; b) Frequency-domain records; (c) Waveform correlation; (d) Wavelet parameters

Bubble pulse amplitude is closely related to gun depth; when the gun depth is smaller than the bubble radius, the bubble will break at the moment of its formation, the gas inside the bubble will escape and the energy will diffuse into the air, and bubble oscillation will not appear. When the gun depth is equal to the bubble radius, since the density of gas inside the bubble is smaller than the density of water, the bubble will rush out of the water under the buoyancy action of water, also leading to bubble breakup, gas escape and energy diffusion. When the gun depth is 1 – 3 times the radius of the bubble, the bubble formed will cause fluctuations of the water surface when it oscillates, which will consume the energy and weaken the bubble oscillation. When the gun depth is greater than 3 times the radius of the bubble, bubble oscillation will be enhanced

with increased gun depth. When a single gun A is fired, the bubble radius is approximately 1m, when the gun depth increases from 8m to 30m, the bubble pulse amplitude shows a generally progressive increasing tendency with the increased gun depth, with a normalized value of 0.95 to 1.40. With gun depth increase, the primary pulse oscillation becomes smaller, the bubble pulse gradually increases, the oscillation of peak-bubble ratio decreases as 13.732 – 28.128, and the normalized value is 0.588 – 1.205. The amplitude of the primary pulse reaches the maximum when the gun depth is 10m, which is consistent with the results by Tang Jie et al. (2009) and Lin Jianmin et al. (2010). At this moment, the peak-bubble ratio is the maximum and can be applied to shallow exploration. As for the deep exploration, the bubble oscillation effect can be enhanced by increasing the gun depth. The bubble pulse amplitude reaches maximum at gun depth of 30m, the amplitude at the depth of 25m is close to that of 30m, but the peak-bubble ratio is the minimum, which can be applied to deep exploration.

With the increase of airgun depth, the bubble oscillation energy gets greater, the bubble oscillating velocity gets faster, and the bubble period is reduced significantly, which is from 0.166s to 0.062s, and the normalized value decreases from 1.000 to 0.373. Accordingly, the dominant frequency in the low-frequency range increases from 6Hz to 10Hz, and the normalized value is from 1.00 to 1.67, presenting a stepped growth. Since the sampling rate of the near-field hydrophone is 1000Hz and the waveform record length is 0.5s, only 500 points are recorded, resulting in a lower frequency domain resolution, but also reflecting the progressive increasing trend of the dominant frequency in the low-frequency range with increased gun depth.

According to the experimental results, the measured peak-bubble ratio and the bubble period are compared with the values normalized using the empirical formulas (formula (2), (3)). The results show the measured peak-bubble ratio reaches its maximum at the gun depth of 10m, then, with the increase of gun depth, the oscillation becomes smaller, which is consistent with the overall trend of the value from formula (2), (3). Both empirical formula derived value and measured value decrease with the increase of gun depth, and the measured value has a greater decreasing range. Meanwhile, using the measured bubble period, the relationship between the bubble period and the gun depth is obtained by fitting as follows:

$$\lg(T) = -1.0771 \lg(D + 10) + 0.5947 \pm 0.0164 \quad (4)$$

$$T = 3.9328 (D + 10)^{-1.0771}, \text{ correlation coefficient } -0.9911 \quad (5)$$

Where, T is the bubble period; D is for the gun depth. The correlation coefficient between bubble period and the gun depth is -0.9911, which further demonstrates that the bubble period and the gun depth are closely related. Fig. 6 is the comparison of the measured airgun wavelet parameters with the values derived from the empirical formulas (formula (2), (3)) and the fitting of bubble period with gun depth.

3.2 Firing Pressure

Firing pressure mainly has impact on the pressure inside the bubble, the greater the firing pressure, the faster the release of gas, and the stronger the wavelet energy of the bubble generated. At first, airgun firing pressure was greater than 6000psi, the operation was very dangerous and would cause great harm to aquatic organisms, so it was difficult to meet the safety and environmental protection requirements. Currently, the generally-used firing pressure is 2000psi.

To explore the influence of firing pressure to the airgun wavelets, we carried out the experiment on the operating conditions of the airgun array with a firing pressure of 1500psi and 2000psi, gun depth of 15m, and water depth of 25m. In each condition, the airgun was shot 9 times, time-frequency filtering was done on the waveforms of each excitation of the airgun array, then the wavelet parameters were averaged and compared after normalization. Table 2 is the near-

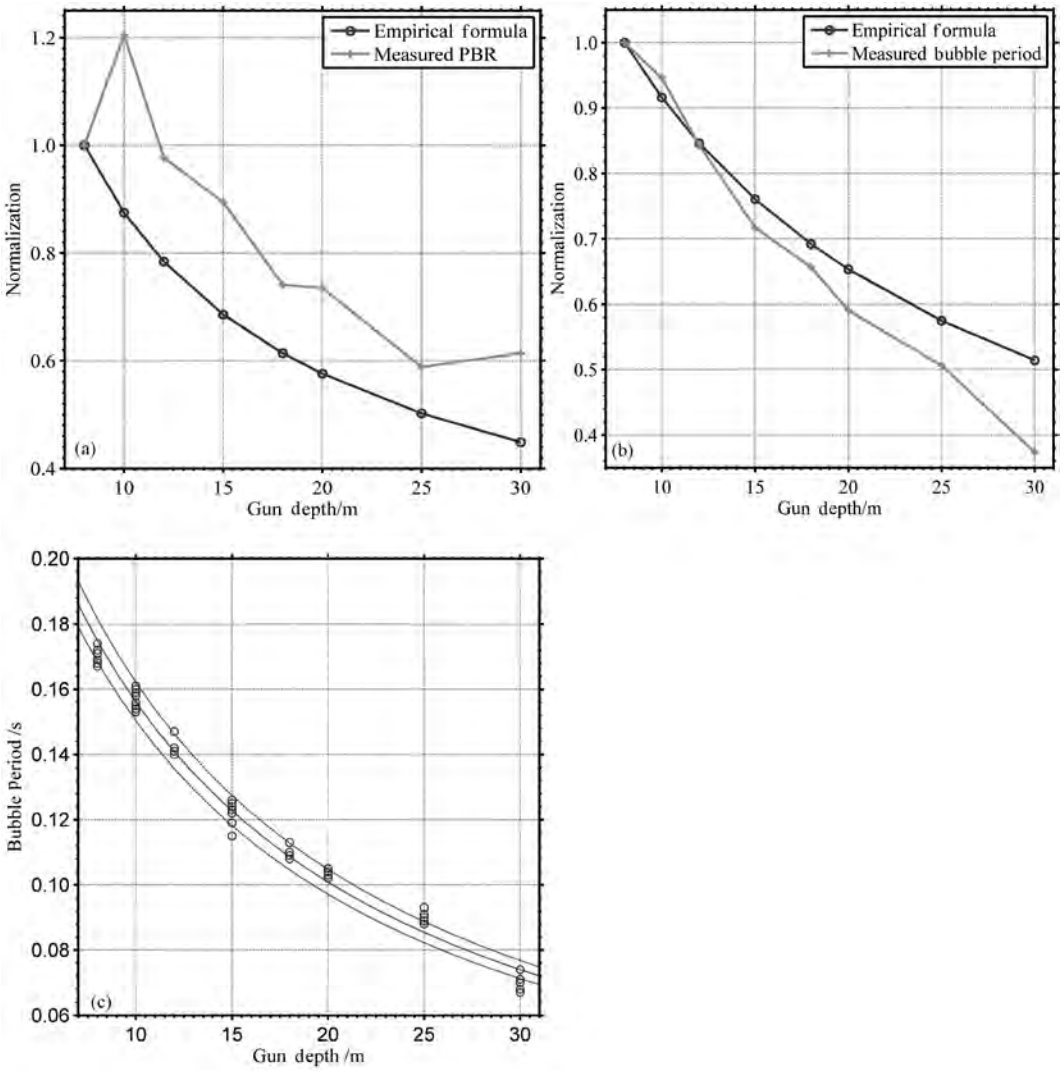

Fig. 6

Comparison of the measured airgun wavelet parameters with the values derived from the empirical formulas and the fitting of bubble period with gun depth

(a) Comparison of the measured airgun peak-bubble ratio with the value derived from the empirical formula (2); (b) Comparison of the measured bubble period with the value derived from the empirical formula (3); (c) The fitting of bubble period with gun depth

field airgun wavelet parameters at different firing pressures. Fig. 7(a) and (b) show the near-field waveform and spectrum of gun A from the first excitation of airgun array. It can be seen that at firing pressure of 2000psi, when the primary pulse amplitude, bubble pulse amplitude and the bubble period are all larger than 1500psi, the first dominant frequency in the low-frequency range remains consistent, for the frequency resolution is not high enough. Fig. 7(c) shows the near-field wavelet waveform correlation comparison under different fringing pressures. We can see that the max cross-correlation coefficient is 0.798 to 1.000 for the primary pulse waveform (the range of 0 – 0.1s), 0.6242 – 1.0000 for the bubble pulse waveform (the range of 0.1 – 0.5s), and 0.7619 – 1.0000 for airgun wavelet waveform (the range of 0 – 0.5s). Correlation of the primary

pulse waveforms at different firing pressures is higher than that of bubble pulse waveform, and the correlation of airgun wavelet is between the primary pulse and the bubble pulse. Fig. 7(d) is the comparison of wavelet parameters after normalization. As it can be seen, when the firing pressure increases from 1500psi to 2000psi, the primary pulse amplitude is increased by 1.07 times, the bubble pulse amplitude increased by 0.352 times, the increasing range of the primary pulse amplitude is larger than that of bubble pulse; Correspondingly, the peak-bubble ratio is increased from 15.67 to 23.98, an increase of 0.53 times, and the bubble period increased from 0.133s to 0.147s, an increase of 0.105 times.

Table 2 Airgun near-field wavelet parameters under different firing pressures

Firing pressure/psi	Wavelet parameters				
	Primary pulse amplitude/count	Bubble pulse amplitude/count	Peak-bubble ratio	Bubble period/s	Dominant frequency/Hz
1500	951.4	60.71	15.67	0.133	6
2000	1968	82.07	23.98	0.147	6

The measured wavelet parameters are compared with the empirical formulas (formula (1), (2), (3)) (Fig. 8). It is clear from Fig. 8 that the increasing range of the measured primary pulse amplitude and the peak-bubble ratio with increased firing pressure is larger than that of the empirical formulas, and the measured bubble pulse amplitude and bubble period have a roughly similar increasing range to that of the empirical formulas.

4 INTERPRETATION OF BUBBLE OSCILLATION MODEL

Johnson (1994) modeled the bubble oscillation process as a pring-damping oscillator and put forward the new interpretation for bubble oscillation using simple physical and mathematical principles (Fig. 9). The resonant water body is equivalent to a spring oscillator, bubble oscillation is equivalent to a spring, and the energy decay in the process of bubble oscillation is equivalent to resistance. The mass of the oscillator is 3 times the mass of the displaced water. According to the formula for the natural vibration period of spring oscillator, we can obtain the bubble period as,

$$\tau = 2\pi R_\infty \sqrt{\frac{\rho_\infty}{3\gamma P_\infty}} \tag{6}$$

The pressure inside the bubble satisfies the equation of state of ideal gas,

$$P_a \frac{4\pi}{3} R^3 \gamma = P_\infty \frac{4\pi}{3} R^3 \gamma_\infty = m \cdot R_g \cdot T \tag{7}$$

namely,

$$P_a = P_\infty \left(\frac{R_\infty}{R}\right)^3 \gamma \tag{8}$$

Where, ρ_∞ is the density of water; P_∞ is hydrostatic pressure; P_a is the pressure inside the bubble; R is the bubble radius; R_∞ is the equilibrium radius of the bubble; m is the mass of air inside the bubble; R_g is the gas constant, for the air, taking $R_g = 287\text{J} / (\text{kg} / ^\circ\text{K})$. T is the temperature inside the bubble; γ is the ratio of specific heat, which is 1.0 under isothermal conditions and 1.4 under adiabatic conditions. Ziolkowski (1970) selected it as $\gamma = 1.13$.

Substituting $P_\infty \frac{4\pi}{3} R^3 \gamma_\infty = m \cdot R_g \cdot T$ into formula(6), we have

$$\tau = \frac{4\pi}{3} \sqrt{\frac{\pi \rho R_\infty^3 \gamma + 2}{\gamma m \cdot R_g \cdot T}} \tag{9}$$

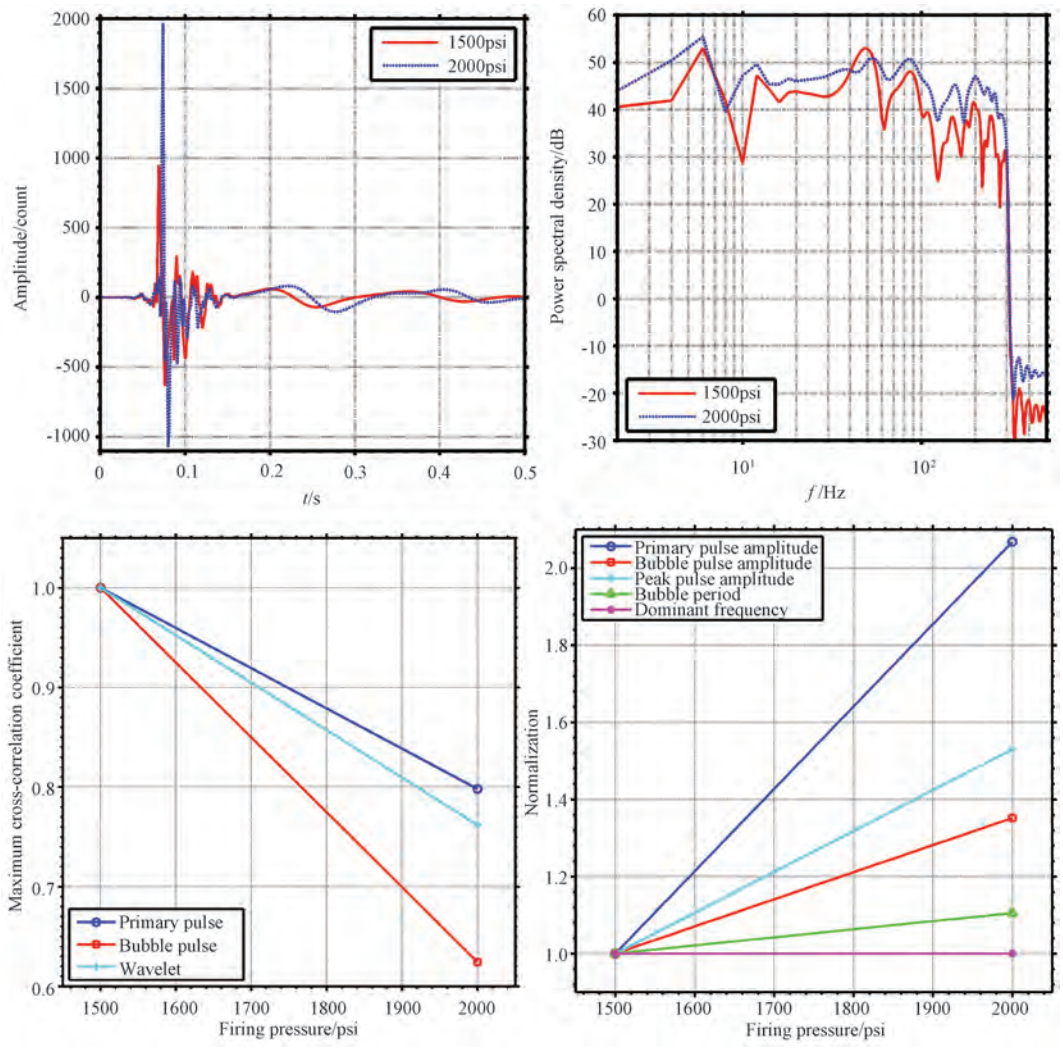

Fig. 7

Analysis of near-field hydrophone recordings at different firing pressures

(a) Time-domain waveform; (b) Spectrum records; (c) Waveform correlation; (d) Wavelet parameters

When airgun capacity and firing pressure are fixed, $m \cdot R_g \cdot T$ is a constant, the greater the gun depth D, the greater the hydrostatic pressure P_∞, the smaller the bubble volume V, and the smaller the equilibrium radius R_∞; Consequently, the bubble period τ obtained by formula (9) decreases and the dominant frequency f in the low-frequency range increases. When airgun capacity and gun depth are fixed, P_∞ is a constant, the firing pressure increases, and the equilibrium radius R_∞ increases too; consequently, the bubble period τ obtained by formula (6) increases and the dominant frequency f in the low-frequency range decreases. This is consistent with the variations of the measured wavelet waveform and spectrum with gun depth and firing pressure.

The corresponding airgun excitation energy is:

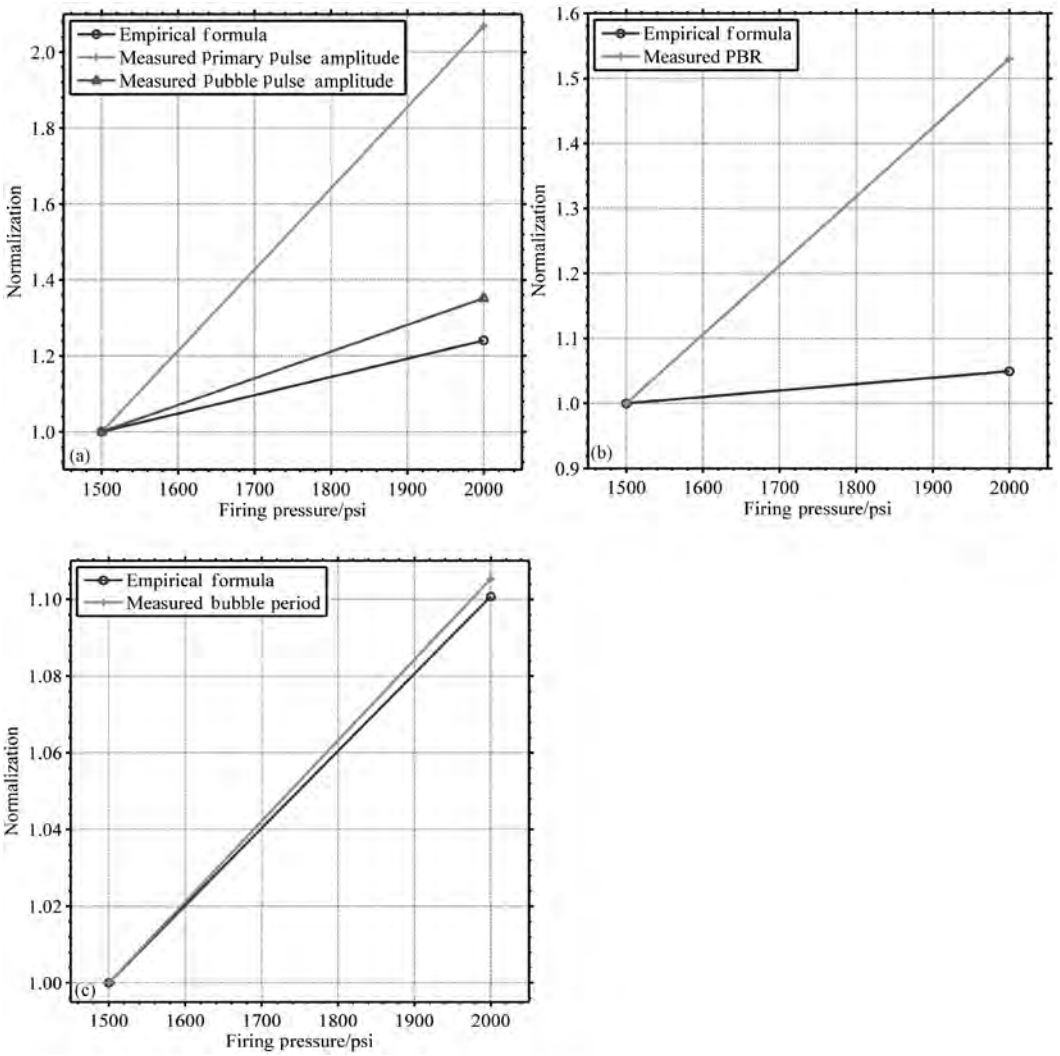

Fig. 8

Comparison of the measured airgun wavelet parameters with the values derived from the empirical formulas under different firing pressures

(a) Primary pulse amplitude and bubble pulse amplitude; (b) Peak-bubble ratio; (c) Bubble period

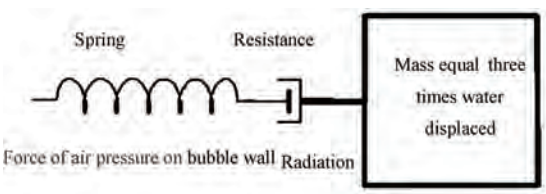

Fig. 9

Bubble oscillation model (after Johnson, 1994)

$$\text{signature} = R(P_a - P_\infty + \frac{\rho_\infty \dot{R}^2}{2}) \tag{10}$$

And the bubble motion equation is:

$$\ddot{R} = \frac{P_a - P_\infty}{\rho_\infty R} - \frac{3\dot{R}^2}{2R} + \frac{1}{\rho_\infty c_\infty}\frac{dP}{dt} \tag{11}$$

Where, R is bubble radius; $\dot{R}$ is the bubble wall velocity; $\ddot{R}$ is the bubble wall acceleration; P_a is the pressure inside the bubble; P_∞ is hydrostatic pressure; ρ_∞ is the density of water, and c_∞ is the velocity of sound in the water. In equation (10), the term $R(P_a\text{-}p_\infty)$ represents the pressure potential energy under the action of pressure inside the bubble and the hydrostatic pressure; $\frac{\rho_\infty \dot{R}^2}{2}$ represents the kinetic energy of the bubble walls in the bubble oscillation. The energy transforms back and forth between the pressure potential energy and the kinetic energy when the bubble is oscillating. In equation (11), $\rho_\infty c_\infty$ represents the impedance of the fluid medium. An acoustic wave propagates in the water, sound energy is radiated outwards from the bubble, $\frac{1}{\rho_\infty c_\infty}\frac{dP}{dt}$ is the sound energy radiation term, and the bubble energy attenuates constantly with the oscillation of bubbles. When the gun depth increases, the hydrostatic pressure P_∞ increases, but the relative pressure P_a inside the bubble is very small at the initial time, so there is small variation in primary pulse amplitudes. When the firing pressure increases, the pressure inside the bubble increases too, the primary pulse amplitude and the bubble pulse amplitude also increase correspondingly. Johnson's model (Johnson, 1994) can explain the variation of the observed wavelet primary pulse amplitude with the gun depth and firing pressure. The change of bubble pulse amplitude versus the increased gun depth is complex, therefore, to improve the bubble model, further research is needed on the dynamics of bubble oscillation, damping mechanism and the impact of boundary conditions, etc.

5 CONCLUSION

High-pressure gas is released into and surrounded by the surrounding water, forming a nearly spherical bubble, and the bubble oscillates continuously in the water until attenuation and breaking, generating a series of wavelet pulses. Airgun wavelet consists of primary pulse and bubble pulse. The primary pulse has large amplitude, short duration time and wide bandwidth, and it is commonly used in shallow exploration. Bubble pulse energy is concentrated in the low frequency range, which penetrates deep vertically and propagates far horizontally, and is commonly used in deep exploration.

The airgun source wavelet is affected by the operating conditions parameters such as gun depth and firing pressure, etc. Gun depth has a direct impact on hydrostatic pressure and water surface ghost reflection, thereby, affecting the release rate of high pressure gas, bubble oscillation effect, wavelet waveform and spectral characteristics. In shallow exploration, since the bubble oscillation will affect the resolution of the signal, it is necessary to enhance the primary pulse, suppress the bubble pulse and broaden the frequency band of the seismic signal. Since the airgun depth is shallow, the bubble energy is weak, the bubble period is long and the wavelet spectrum is relatively smooth. Meanwhile, taking advantage of coherence and resonating function between the bubbles, and by adjusting the assemblage of different airgun arrays to weaken the bubble

oscillation, the bubble pulse amplitude is reduced, thereby a smooth broadband can be obtained and the shallow detection resolution enhanced. By analyzing the airgun near-field hydrophone waveform records in the Jiemian reservoir, it is found that the primary pulse amplitude and peak-bubble ratio are at the maximum at the gun depth of 10m, which can be applied to shallow exploration.

In deep exploration, it is required to enhance the bubble pulse energy, increase the low-frequency components of the wavelet, as well as increasing the penetration depth and seismic wave propagation distance. The deeper the gun depth, the more intensive the bubble oscillation will be, and the stronger the wavelet energy, the smaller the bubble period; the dominant frequency in the low-frequency range will also increase correspondingly. Meanwhile, the deeper the gun depth, the smaller the notch frequency caused by water surface ghost reflection; the pass-band of the airgun wavelet will become narrower, and the center frequency will shift to lower frequencies, which will have a suppression effect on the airgun wavelet energy. So, in deep exploration, we need to select the appropriate gun depth and take into account the demands of low frequency and energy, and when necessary, these issues need to be determined through field experiments. By analyzing the waveform records of the airgun source experiment in the Jiemian reservoir, it is found that the peak-bubble ratio reaches its peak at gun depth of 25m, which can be used in deep exploration.

Firing pressure mainly affects the pressure inside the bubble. The greater the firing pressure, the faster the release rate of gas, and the stronger the bubble wavelet energy produced. With the increased firing pressure, the increasing range of primary pulse amplitude is greater than the bubble pulse amplitude, and the peak-bubble ratio and the bubble period are increased correspondingly.

Study of the time-frequency characteristics of airgun wavelets and the impact from gun depth and firing pressure will help us adjust the excitation parameters and select the optimum operating conditions according to the different requirements of source excitation signals for different detection targets, so as to obtain the best excitation effect.

REFERENCES

Brenguier F., Campillo M., Hadziioannou C., et al. Postseismic relaxation along the San Andreas Fault at Parkfield from continuous seismological observations [J]. *Science*, 2008, 321: 1478 – 1481.

He Hanyi. *The Offshore High-resolution Seismic Prospecting Techniques and Its Application* [M]. Beijing: Geological Publishing House, 2001. 1 – 129 (in Chinese).

Johnson D. T. Understanding airgun bubble behavior [J]. *Geophysics*, 1994, 59(11): 1729 – 1734.

Lin Jianmin, Wang Baoshan, Ge Hongkui et al. Characters of large volume airgun source excitation [J]. *Chin J Geophys*, 2010, 53(2): 342 – 349 (in Chinese with English abstract).

Lin Jianmin. *Long-offset Seismic Signal Detection and Exploration with Active Source* [D]. Doctoral thesis. Hefei: University of Science and Technology of China, 2008 (in Chinese with English abstract).

Luo Guichun, Wang Baoshan, Ge Hongkui et al. Progress in earth's deep structures exploration by airgun source [J]. *Progress in Geophysics*, 2006, 21(2): 400 – 407 (in Chinese with English abstract).

Okaya D. A, Henrys S., Stem T. Double sided onshore-offshore seismic imaging of a plate boundary: "super-gathers" across South Island, New Zealand [J]. *Tectonophysics*, 2002, 355: 247 – 263.

Qiu Xuelin, Zhao Minghui, Ye Chunming et al. Ocean bottom seismometer and onshore-offshore seismic experiment in north- eastern South China Sea [J]. *Geotectonica et Metallogenia*, 2004, 28(1): 28 – 35.

Tang Jie, Wang Baoshan, Ge Hongkui et al. Experiment and simulation of large capacity airguns in deep structure exploration [J]. *Earthquake Research in China*, 2009, 25(1): 1 – 10 (in Chinese with English abstract).

Tang Jie. *Study on Active Character and Weak Signal Detection in Regional Scale Deep Exploration* [D]. Doctoral thesis. Hefei: University of Science and Technology of China, 2008 (in Chinese with English abstract).

Wang Baoshan, Wang Weijun, Ge Hongkui et al. Monitoring subsurface changes with active sources [J]. *Advances in Earth Science*, 2011, 26(3): 249 – 256 (in Chinese with English abstract).

Wang Baoshan, Yang Wei, Wang Weitao et al. *Monitoring the Change of Crust Medium in North Tianshan Using Large-volume Airguns* [C]. In: Chinese Geophysical Society, the Chinese Geophysics 2013—Special Topic No. 12, 2, 2013.

Wang Weitao. *Study on the Detection of Regional Scale Medium Wave Velocity Based on Artificial Source* [D]. Doctoral thesis. Hefei: University of Science and Technology of China, 2009 (in Chinese with English abstract).

Woods H. Los Angeles region seismic experiment (LARSE) – cruise report, 1995.

Yang Wei, Wang Baoshan, Ge Hongkui et al. The active monitoring system with large volume airgun source and experiment [J]. *Earthquake Research in China*, 2013, 29(4): 399 – 410 (in Chinese with English abstract).

Yang Wei. *Technology and Experimental Study of Regional Scale Active Source Detection* [D]. Doctoral thesis. Beijing: Institute of Geophysics, China Earthquake Administration, 2013 (in Chinese with English abstract).

Ziolkowski A. A method for calculating the output pressure waveform from an airgun [J]. *Geophys J Roy Astr Soc*, 1970, 21: 137 – 161.

About the Author

Xia Ji, born in 1988, is a doctoral student at the Institute of Engineering Mechanics, CEA. His major is the study of the detection of active sources. E-mail: xiaji992007@126.com